19th Australasian Fluid Mechanics Conference
Melbourne, Australia
8-11 December 2014

# Two and Three Dimensional Stability Analysis of an Optimum Glauert Rotor at Low Reynolds Number

**D. M. Smith, H. M. Blackburn and J. Sheridan**

Department of Mechanical and Aerospace Engineering
Monash University, Clayton 3000 Victoria, Australia

## Abstract

Turbines in farm operation are subject to adverse operating conditions when operating in the wake of one or more upstream turbines. The stability of a turbine wake is important in this consideration, where an understanding of instability mechanisms could yield performance gains. Owing to the scale of large wind farms, axisymmetric models are often employed to model performance. In this study we use actuator Navier–Stokes methods to produce three and two-dimensional axisymmetric wakes of a wind turbine and compute instability modes directly from a direct numerical simulation (DNS). For axisymmetric computations, modes are axisymmetric only, and three dimensional wakes consider three dimensional instability modes. An axisymmetric base flow was found to be less stable than an equivalent three dimensional computation, and all cases studied between Reynolds numbers of 300 and 3000 were found to be stable. Similar mode shapes between two and three dimensional computations were found for least stable modes at the Reynolds numbers considered.

## Introduction

Horizontal axis Wind turbines (HAWT) are increasingly deployed in farm configurations to minimize total installed cost of energy. Thus, increasing emphasis is being placed on the wake region of a turbine, as this forms the inflow condition for many turbines downstream of the leading rotor(s).

The higher turbulence intensity and lower flow speeds of a turbine wake are undesirable for wind farms. Higher turbulence intensity contributes to a lower fatigue life of a turbine. Lower flow speeds reduce energy output. For low freestream turbulence intensity, leading turbine wakes travel further into the wind farm and more strongly influence flow for downstream turbines. Study of the Vindeby offshore wind farm in [4] found that the effects of a turbine wake on fatigue loading were similar to a wind direction that was incident over land. Another study in [12] concluded that wake effects were more prominent for turbines when ambient turbulence intensity was low. A study in [2] found similar outcomes.

Findings that the turbulence generated by a turbine can have significant effects motivates studies of turbine wakes. The wake of an individual N-bladed turbine was first described by Joukowski in [9] as a system of N+1 helical vortices, with N helical tip vortices and one single hub vortex. The model for the helical tip vortices was later used by Widnall in [14] which was the first successful study of the stability for helical vortex filaments. Widnall's work identified that the system was least stable to long wave disturbances, particularly those that moved streamwise adjacent elements of the filament closer together. These findings have been reproduced in more sophisticated computations such as those by Walther in [13], as well as by methods that include a model for the turbine in [7]. The findings have also been observed experimentally in [3]. More recent works have also tried to integrate observations for instability growth rates into estimates for the wake length of a turbine in [3].

A common practice to excite the long and short wave instabilities in a helical vortex filament is to prescribe a set of harmonic disturbances at the blade tip, which may have the unintended drawback of only highlighting these mechanisms. The work presented here avoids harmonic excitement by computing modes and stability properties by examining flowfields from a DNS computation of a stable flow. To put the work in context, results for three-dimensional modes and growth rates are compared to modes that result from an axisymmetric model for the turbine that is often employed in studies of large wind farms.

## Methodology

### Optimum Rotor and Problem Definition

Base-flows are computed using an actuator Navier–Stokes method where body forces are added to a Navier–Stokes solver to reproduce turbine dynamics. Body forces are determined from a prediction of turbine loading, usually from tabulated aerofoil data. The forces are then smoothed locally in the domain according to equation 1, with $F_{2D}$ describing the desired force, $d$, the orthogonal distance to the blade line and $\varepsilon$ controlling the size over which the forces are applied. A more detailed description of the method is available in [8].

It should be noted that the actuator line model is one of several methods to reproduce turbine dynamics using body forces. An alternative to smoothing the forces in the region of the blades is to instead smooth over the entire swept area of the blade. The resulting axisymmetric force description is computationally more efficient as base flows are two-dimensional and therefore this method has been used to validate our description of a Glauert optimum rotor.

$$\mathbf{f}(d,r,z) = \frac{F_{2D}}{\pi\varepsilon^2}\exp\left(\frac{d^2}{\varepsilon^2}\right) \tag{1}$$

$$\frac{\partial \mathbf{u}}{\partial t} = \frac{-1}{\rho}\nabla p + \nu\nabla^2\mathbf{u} - \mathbf{u}\cdot\nabla\mathbf{u} + \mathbf{f} \tag{2}$$

To model an optimum rotor, rather than specify a turbine geometry and aerofoil profile, the product of chord and either normal or tangential coefficient is scaled with the local dynamic pressure to arrive at forcing, $F_{2D}$ either normal or tangential to the blade swept area. Blade normal and tangential force coefficients; $cC_N$ and $cC_T$ are determined by coupling Blade Element Momentum theory described in [6] with an inviscid optimum rotor [5]. An inviscid optimum rotor is produced by optimizing axial and tangential induction factors $(a, a')$ given by 3 according to optimization conditions in 4.

$$a = 1 - \frac{u}{U_\infty} \qquad a' = \frac{w}{\Omega r} \tag{3}$$

$$\max\left(a'(1-a)\right) \qquad a' = \frac{1-3a}{4a-1} \tag{4}$$

Once optimum induction factors are known in accordance with an optimum Glauert rotor, the local angle of attack, $\phi$ can be determined and therefore the product of chord and either normal or tangential forcing coefficient described by eq. 7. Here, $\Omega$ denotes the blade rotation rate, tip speed ratio, $\lambda = \Omega R/V_\infty$ and $r$ is the radial distance from the axis of rotation for the blade.

$$\phi = \arctan\left(\frac{1-a}{1+a'}\Omega r\right) \tag{5}$$

$$cC_N = \frac{4F\sin^2\phi}{\frac{B}{2\pi r}(\frac{1}{a}-1)} \tag{6}$$

$$cC_T = \frac{4F\sin\phi\cos\phi}{\frac{B}{2\pi r}(\frac{1}{a'}+1)} \tag{7}$$

In our description of the base flow, Prandtl's tip loss factor, $F$ is used to account for three dimensional effects at the blade tip and is given by eq. 8, where the number of turbine blades, $B$ is three.

$$F = \frac{2}{\pi}\cos^{-1}\left(\exp\frac{-B(R-r)(1+\lambda^2)^{-0.5}}{2R}\right) \tag{8}$$

Forcing coefficients for an optimum rotor were applied using an actuator disc model for the turbine to produce velocity profiles at the rotor. The resulting streamwise velocity profiles are shown in figure 1 which shows a comparison between flow at the rotor and the inviscid prediction for various Reynolds numbers. The agreement is generally within 5% and improves with increasing Reynolds number. The test was repeated using an actuator line model, where turbine loading agreed within 5% of an equivalent disc computation as well.

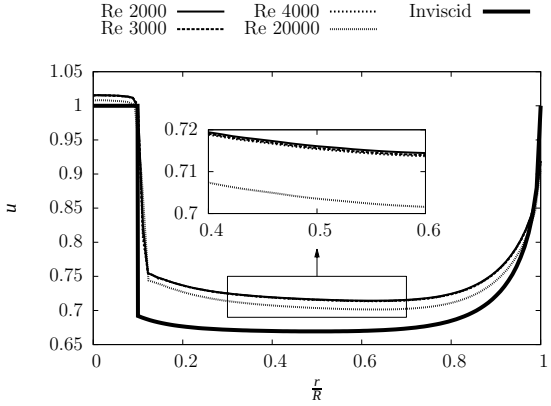


Figure 1: Streamwise velocity at the rotor plane for Reynolds numbers between 2000 and 20000, showing comparison between the inviscid prediction of streamwise velocity $(u)$ at the rotor and outcomes from an actuator disc simulation. $r$ denotes distance radially away from the turbine axis of rotation and $R$ is the turbine radius. Results agree within 5% and improve with increasing Reynolds number

Using the actuator line model, with forcing consistent with a Glauert rotor, base flows have been generated for various Reynolds numbers, here defined according to the freestream velocity $U_\infty$ and the blade radius, $R$ of unity. For all results to be presented, a turbine design tip speed ratio of 4 was considered. Computations take place on a computational domain with a spectral element Navier–Stokes Solver with Fourier modal description over azimuth described by [1]. The mesh, a meridional semiplane in cylindrical coordinates with Fourier projection over azimuth consisted of 2593 spectral elements.

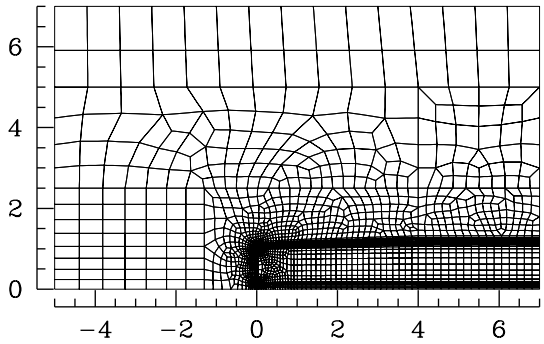

Figure 2: Computational domain showing spectral element meridional semiplane used for the study. Flow is from left to right, with Dirchlet velocity inflow and Neuman outflow boundary conditions. Bottom edge of the domain represents the axis of rotation for the turbine, where an axis boundary condition has been used. The top boundary is free slip for streamwise velocity and Dirchlet for radial and azimuthal velocity components

For both axisymmetric and three-dimensional computations the element polynomial order was 6, and for three dimensional cases 16 Fourier modes were employed for a reduced 120 degree wedge domain in azimuth with periodic boundary conditions to model a three bladed rotor. The meridional semiplane domain is shown by figure 2. Computations are performed in a rotating reference frame which produces steady wake structures for three dimensional cases, rather than periodic as tip vortices rotate at the same speed as the reference frame. The upstream, radial and downstream lengths are 5, 7 and 7 rotor lengths respectively.

Computations for stability analysis have been carried out for a turbine at design tip speed ratio of 4 for Reynolds numbers between 500 and 3000. An example computation for a three-dimensional flow is given by figure 3 at a Reynolds number of 2000 and serves to highlight helical vortex structures associated with shed vorticity at the blade root and tip that are of interest in this study. For a two dimensional computation the helical vortices become shear layers.

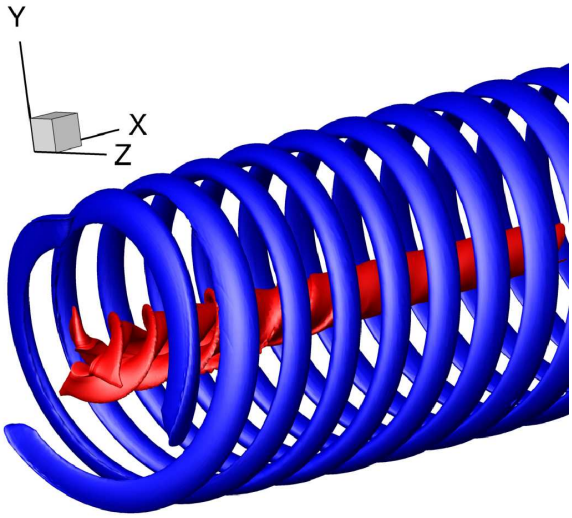


Figure 3: Wake structures from an actuator line computation at Reynolds number 2000 and tip speed ratio of 4. Blue and red isosurfaces highlight the helical vortex structures.

## Stability Analysis

The stability analysis presented here is based on the residual algorithm outlined by [11], and uses time history of a point in space, $x$ for a linearly stable DNS computation where the flow-field, $U$ is described by $\lim_{t\to\infty} u(x,t) = U(x)$. If the flow is perturbed with small scale amplitude and evolved forwards in time, the flow evolution is described by the sum of the first n eigenmodes in eq 9. For our computations, perturbations arise from a non equilibrium initial condition.

$$u(x,t) = U(x) + \sum_n \hat{u}_n(x) e^{\lambda_n t} + c.c. \tag{9}$$

For a linearly stable flow, and large time since the linear perturbation, the amplitude of all modes except the least stable will decay. Where only the least stable mode is active, $u(x,t)$ is described by only one mode in eq. 9.

The first eigenvalue can be determined from eq 9 using the time history for the flow velocity at a sample location, $u_x(t)$. For two samples of the flow: $u_x(t), u_x(t+\Delta t)$, then:

$$u_x(t) = U(x) + \hat{u}_1(x) e^{\lambda_1(t)} \tag{10}$$

$$u_x(t+\Delta t) = U(x) + \hat{u}_1(x) e^{\lambda_1(t+\Delta t)} \tag{11}$$

by using equation 11 it can be shown that the residual, $\log\left(\left|\frac{u_x(t+\Delta t - u_x(t)}{\Delta t}\right|\right)$ is a linear function with slope equal to the real part of the eigenvalue. Where the leading mode is complex, the residual shows oscillatory behavior. In either scenario a linear curve fit to the residual indicates growth rate, and periodicity in the residual is proportional to the imaginary part of the leading eigenvalue. For computations where the leading eigenmode is real, mode shapes can be approximated according to: $\hat{u}(x) = u(x,t+\Delta t) - u(x,t)$.

### Results and Discussion

Growth rates were found for actuator line computations at Reynolds numbers ranging between 300 and 2500, as well as for actuator disc computations at Reynolds numbers between 500 and 2000. As a first consideration, only axisymmetric perturbations were considered for the actuator disc computations as [10] identified that the least stable perturbations were axisymmetric, however the study was limited to a Reynolds number of 500. Given the three-dimensional nature of the simulations for actuator line cases, the modes arising from such computations are three-dimensional in nature. A summary of the observed growth rates for three-dimensional perturbations to an actuator line computation as well as two-dimensional perturbations to an actuator disc computation is shown by figure 4, which identifies that the axisymmetric wake is less stable than for an equivalent three dimensional computation.

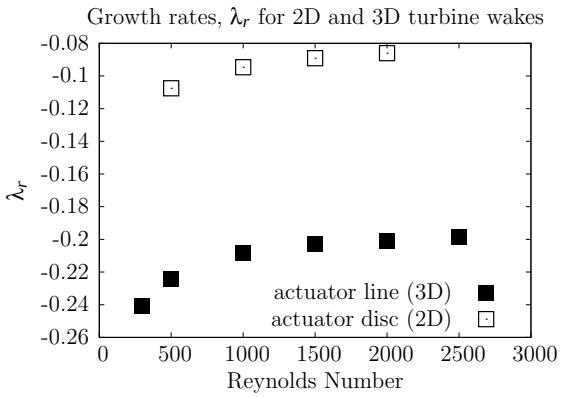


Figure 4: Comparison of least stable growth rates for actuator line and actuator disc base flow computations for various Reynolds numbers.

Eigenvalues for both actuator line and actuator disc computations show real only eigenvalues at Reynolds numbers below 2000, but periodicity becomes evident in the residual at Reynolds numbers of 2000 and above, indicating a change in perturbation structure at these Reynolds numbers. Mode shapes for these computations are yet to be identified and will be considered in further work.

Mode shapes were identified for base flow computations where real only eigenvalues were observed. Given the actuator line computations are in a rotating reference frame, real only eigenvalues indicate that the least stable mode moves with blade rotation and vortices downstream of the rotor.

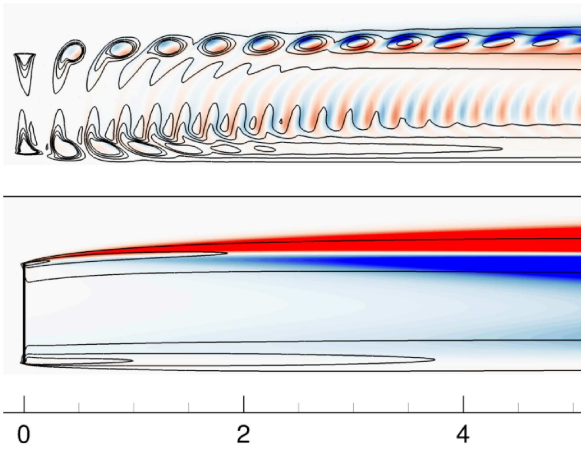


Figure 5: Least stable mode shape at Reynolds number 1500 shown using contours of azimuthal vorticity (blue negative, red positive) over a meridional semiplane for the least stable mode at Re 1500. Top shows the mode identified for the actuator line simulation and the bottom shows the actuator disc result for the same parameters. Overlaid is black contour lines of azimuthal vorticity the base flow computation. The rotor is located at the far left of the figure, and highlighted with a solid line for the actuator disc computation.

At Reynolds numbers below 2000, mode shapes have been identified and are consistent with figure 5. For both the actuator line and disc computations, the least stable modes are best shown according to azimuthal vorticity contours, and align closely with the vortex structure for actuator line computations, or the tip shear layer in the case of an actuator disc computation. Least stable modes for actuator line computations, appear as a counter rotating vortex pair within the tip vortices themselves, and suggest that viscous effects at this low Reynolds number act to damp out mutual inductance type modes, and instead line vortex instabilities dominate. Mode shapes for an actuator disc computation appear to be related to the same dynamics, and appear as a pair of opposing vorticity, but is instead smeared over the cylindrical sheet of vorticity that produces the shear layer for an actuator disc computation. Owing to the larger surface area of such an arrangement it appears to be more easily disrupted than for an equivalent actuator line computation.

#### Conclusions

Two-dimensional and Three-dimensional turbine wake stability was investigated at low Reynolds number. Stability properties were estimated from the base flow computation and considered three dimensional perturbations to an actuator line simulation, as well as two dimensional perturbations to an axisymmetric actuator disc simulation. The study found that the two dimensional wake computed by the actuator disc model was less stable than an equivalent actuator line computation. Flow physics between the two simulations showed similarities, with a counter rotating azimuthal vortex pair identified for the actuator line simulation which appeared as a streak like structure over the shear layer produced by an actuator disc computation. . Further work will expand the Reynolds numbers under consideration and also calculate non-axisymmetric perturbations to the two dimensional wake structure for the actuator disc model.

#### References

[1] Blackburn, H.M. and Sherwin, S.J., Formulation of a galerkin spectral element-fourier method for three-dimensional incompressible flows in cylindrical geometries, *J. computational physics*

[2] Dahlberg, J.Å., Poppen, M., Thor, S.E., Wind farm load spectra based on measurements. *EWEA Special topic conference 92: The potential of wind farms*, 1992.

[3] Felli, M., Camussi, R., Di Felice, F., Mechanisms of evolution of the propeller wake in the transition and farfields. *J. fluid mechanics*, 2011, 1-49.

[4] Frandsen, S. and Christensen, C.J., Vindeboy Offshore Wind Farm Fatigue Loads, *European wind energy conference and exhibition*, 1995.

[5] Glauert, H. Airplane Propellers, *Springer Berlin Heidelberg*, 1935.

[6] Hansen, O.H., *Aerodynamics of wind turbines*, Earthscan, 2008.

[7] Ivanell, S., Mikkelsen, R., Sørensen, J.N., Henningson, D., Stability analysis of the tip vortices of a wind turbine, *J. wind energy* **12**, 2010.

[8] Ivanell, S., Sørensen, J.N., Mikkelsen, R. and Henningson, D. Analysis of numerically generated wake structures *J. wind energy* **12**, 2009, 63-80.

[9] Joukowski, N.E., Vortex theory of a rowing screw *Trudy otdeleniya fizicheskikh nauk obshchestva lubitelei estestvoznaniya* **16**, 1912

[10] Smith, D.M., Blackburn, H.M., Sheridan, J., Linear stability analysis for an optimum glauert rotor modelled by an actuator disc. *J. physics conference series* **524**, 2014.

[11] Theofilis, V. On steady-state flow solutions and their non-parallel global linear instability. *Advances in turbulence VIII*, 2000.

[12] Thomsen, K. and Sørensen. P., Fatigue loads for wind turbines operating in wakes *J. Wind Engineering and Industrial Aerodynamics*, **80**, 1999, 121-136.

[13] Walther, J.H., Guenot, M., Rasmussen, E.T., Chatelain, P., Okulov, V.L., Sørensen, J.N., Bergdorf, M., Koumoutsakos, P., A numerical study of the stability of helical vortices using vortex methods. *J. physics: Conference series* **75**, 2007.

[14] Widnall, S.E. and Sullivan, J.P., On the stability of vortex rings *Proceedings of the royal society of London A. mathematical and physical sciences* **332**, 1973, 335-353.